J. Astrophys. Astr. (1988) **9**, 231–236

One more Explanation of Superluminal Motion

V. Krishan *Indian Institute of Astrophysics, Bangalore 560034*

Received 1988 July 11; accepted 1988 October 14

Abstract. The occurrence of superluminal motion in extragalactic radio sources is believed to be quite common. Among others, the geometrical scattering of radio radiation can also cause superluminal expansion and or motion and halo formation. In this paper, the effectiveness of the stimulated Raman scattering in producing these features is investigated. The scattering medium is a plasma whose position, density and temperature decide the rate and angle of scattering. When the radiation from a stationary and constant source gets scattered from a stationary plasma, a halo is formed around the source. However, the scattering of a rotating radiation beam does produce superluminal motion of the virtual source. It is found that the plasma should have the characteristics of the emission-line regions and the intercloud medium in order to Raman scatter the radiation. Since the scattering is polarization dependent, it is possible to estimate the rotation of the electric vector along the direction of the apparent motion of a radio source.

Key words: extragalactic radio sources—superluminal motion—Raman scattering

1. Introduction

The several explanations of superluminal motion include: (i) a light house model in which a small change in the direction of electromagnetic beam causes a large traversal on a distant screen, exciting it in the process; (ii) relativistic beaming in which the source moving at a small angle to the line of sight with a speed slightly less than the speed of light, appears to move with superluminal speeds perpendicular to the line of sight due to light travel time effects (Blandford, McKee & Rees 1977; Blandford & Königl 1979); (iii) gravitational lensing which can magnify the real motion and the observed flux (Barnothy 1965). A critical discussion of these processes can be found in Scheuer (1984). Sanders (1974) used geometrical effects of a strong dipole magnetic field to account for superluminal expansion, though it is infested with the fast fall of flux with separation as pointed out by Blandford, McKee & Rees (1977). Wilson (1982) considered induced Compton scattering which though can give rise to light-echo effects and therefore superluminal motion but the strong frequency dependence of the motion is in contradiction with the observations. Here, we consider stimulated Raman scattering of radio radiation in a plasma such that the apparent motion of the source is actually the scattered radiation at increasing scattering angles. The advantages of this coherent scattering process are the preservation of the flux and its spectral characteristics after the scattering, provided the plasma parameters are chosen appropriately.

2. Stimulated Raman scattering in superluminal sources

Consider a large-amplitude plane-polarized electromagnetic wave $\mathbf{E}_0 = 2E_0\hat{\mathbf{e}}_0\cos(\mathbf{K}_0\cdot\mathbf{x}-\omega_0 t)$ incident on a plasma of electron density n and temperature T. Stimulated Raman scattering takes place when the incident wave $(\omega_0, \mathbf{K}_0)$ decays into a scattered wave $(\omega_s, \mathbf{k}_s)$ and an electron plasma wave $(\omega_e, \mathbf{K}_e)$ such that

$$\omega_0 = \omega_s + \omega_e,$$
$$\mathbf{K}_0 = \mathbf{K}_s + \mathbf{K}_e. \tag{1}$$

The equilibrium consists of electrons oscillating with velocity $V_0 = eE_0/m\omega_0$ in the field of the incident wave. Ions form a stationary background. Raman scattering is a nonlinear process and occurs when the incident radiation satisfies a threshold condition (Krishan 1988; Drake *et al.* 1974):

$$\left(\frac{V_0}{c}\right)^2 \geqslant \frac{1}{\psi^2}\left(\frac{\Gamma_p}{\omega_p}\right)\left(\frac{\Gamma_-}{\omega_0}\right) \tag{2}$$

where

$$\psi = |\sin\phi|\cos\theta_e,$$
$$\sin^2\phi = \frac{\mathbf{E}_0\cdot\mathbf{E}_s}{|E_0||E_s|},$$

and $\phi = \pi/2$ when the incident $\mathbf{E}_0$ and scattered $\mathbf{E}_s$ waves are polarized in the same direction; θ_e is the angle between $\mathbf{K}_0$ and $\mathbf{K}_e$,

$$\Gamma_p = \frac{\sqrt{\pi}}{2}\frac{\omega_p}{K_e^3\lambda_D^3}\exp\left[-\frac{1}{2K_e^2\lambda_D^2}-\frac{3}{4}\right]+\gamma_{ei} \tag{3}$$

is the damping rate of the electron plasma wave, and

$$\gamma_{ei} = (3\omega_p/4\pi n\lambda_D^3)$$

is the electron-ion collision frequency; $\Gamma_- = (\omega_p^2\gamma_{ei}/2\omega_s^2)$ is the collisional damping rate of the electromagnetic wave of frequency ω_s; $\omega_p = (4\pi ne^2/m)^{1/2}$ is the electron plasma frequency, λ_D is the Debye length. The maximum growth rate for stimulated Raman scattering is found to be:

$$\gamma_{sR} = \frac{V_0}{c}\psi(\omega_0\omega_p)^{1/2}$$

for $\omega_p \gg \gamma_{sR} \gg \Gamma_p$ and $V_0/c > \Gamma_p/(\psi\omega_0\omega_p)^{1/2}$. In the above analysis $\omega_0 \gg \omega_e \simeq \omega_p$ and therefore $\omega_0 \simeq \omega_s$; $\omega_0 = K_0 c$, $K_e = 2K_0\cos\theta_e$ and $K_e\lambda_D < 1$ so that the electron plasma wave is only weakly damped. The threshold condition (2) is rewritten as:

$$(\omega_0)\left(\frac{L_{47}}{r_{pc}^2}\right) \geqslant \frac{2.85\times10^7 n_{10}^{1/2}(\omega_0/\omega_R)^{\alpha-1}}{\cos^2\theta_e\sin^2\phi\, T_4^3}\times$$
$$\times\left[\frac{2.67\times10^{39}n_{10}^3}{\cos^3\theta_e\,\omega_0^3}\exp\left\{-\frac{1.19\times10^{24}n_{10}}{\omega_0^2\cos^2\theta_e T_4}-\frac{3}{4}\right\}+2.31\times10^{-2}n_{10}^2\right]. \tag{4}$$

The conditions $K_e\lambda_D<1$ and $\omega_0 \gg \omega_p$ translate to

$$5.46\times10^9 n_{10}^{1/2} \ll \omega_0 < \frac{1.54\times10^{12}}{\cos\theta_e} n_{10}^{1/2} T_4^{-1/2}. \tag{5}$$

Here, $L=L_{47}\times10^{47}$ erg s^{-1} is the luminosity of radio radiation and $R=r_{pc}\times 3\times10^{18}$ cm is the position of the scattering plasma of density $n=n_{10}\times10^{10}$ cm^{-3} and temperature $T=T_4\times10^4$ K. α is the radiation spectral index such that the flux $F_\omega\propto\omega^{-\alpha}$, then the spectral variation of the luminosity $L_{47}(\omega)$ is given as:

$$L_{47}(\omega_0)=L_{47}(\omega_R)\left(\frac{\omega_0}{\omega_R}\right)^{-\alpha+1}$$

and the energy density $E_0^2(\omega_0)$ can be expressed as:

$$E_0^2(\omega_0)=\frac{0.37\,L_{47}(\omega_0)}{r_{pc}^2}=\frac{0.37}{r_{pc}^2}\,L_{47}(\omega_R)\left(\frac{\omega_0}{\omega_R}\right)^{-\alpha+1}$$

where ω_R is a reference frequency. Equation (4) describes the variation of luminosity as a function of the angle θ_e which is related to the scattering angle $\theta_s=\cos^{-1}[\mathbf{K}_0\cdot\mathbf{K}_s/(|K_0||K_s|)]$ as, $\cos\theta_s=1-2\cos^2\theta_e$, for given plasma parameters, when the incident radiation has attained a steady state with the plasma. It is known that the maximum allowed value of $K_e\lambda_D\sim0.4$ for Raman scattering to remain valid. This gives the highest allowed frequency of the incident radiation as:

$$\omega_0|_{max}=\frac{6.17\times10^{11}\,n_{10}^{1/2}\,T_4^{-1/2}}{\cos\theta_e}\ \text{s}^{-1} \tag{6}$$

3. Superluminal motion

The superluminal sources generally show a core and jet configuration. The jet and features in it like knots show superluminal motion with respect to the core. In the case of radiation from a stationary source scattered by stationary plasma surrounding the source, since one does not observe a time delay between the direct and the scattered paths of the radiation, the formation of virtual images for different angles of incidence results in a halo around the source. Motion may appear to take place if the source is a delta function in time and the plasma is localized along a line perpendicular to the line of sight. The apparent superluminal motion of the jet can result if source radiation beam, the fixed end of which is in the core is rotating. Let us imagine a ring of plasma ($P_1P_2\ldots$) at a distance of about one pc from the core A. The rotating radiation beam intercepts plasma at increasing angles ($P_1P_2\ldots$) as it rotates (say anticlockwise in Fig. 1). To an observer at M the Raman scattered radiation appears to come from $A_1\ A_2\ldots$ at successive times. The observed motion of a few milliarcseconds per year of ($A_1A_2\ldots$) corresponds to a rotation rate $\frac{d\theta}{dt}=\left(\frac{\text{mas}}{\text{yr}}\right)\frac{PM}{AP}\simeq10^3$ arcsec yr^{-1} of the beam (AP_1, $AP_2\ldots$). The apparent motion takes place with a uniform speed if the beam rotates at a uniform rate. From Fig. 1, the scattering angle θ_s is given as $\theta_s\simeq180-\theta$ and recall that $\cos\theta_s=1-2\cos^2\theta_e$.

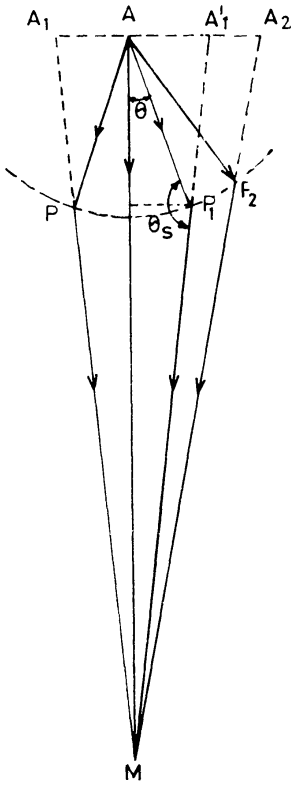

Figure 1. Apparent superluminal motion of radio source A through geometrical scattering.

As θ increases, θ_s decreases and so does $\cos\theta_e$. The variation with $\cos\theta_e$ of threshold for Raman scattering is shown in Fig. 2. The threshold is found to be the lowest for θ_e between 30°–60° which corresponds to θ between 64°–127°. Thus for a given value of θ and θ_s, θ_e can be calculated and so can be the steady state value of (L_{47}/r_{pc}^2). In Fig. (3) (ω_0) (L_{47}/r_{pc}^2) is plotted against frequency for two values of θ for different sets of fixed

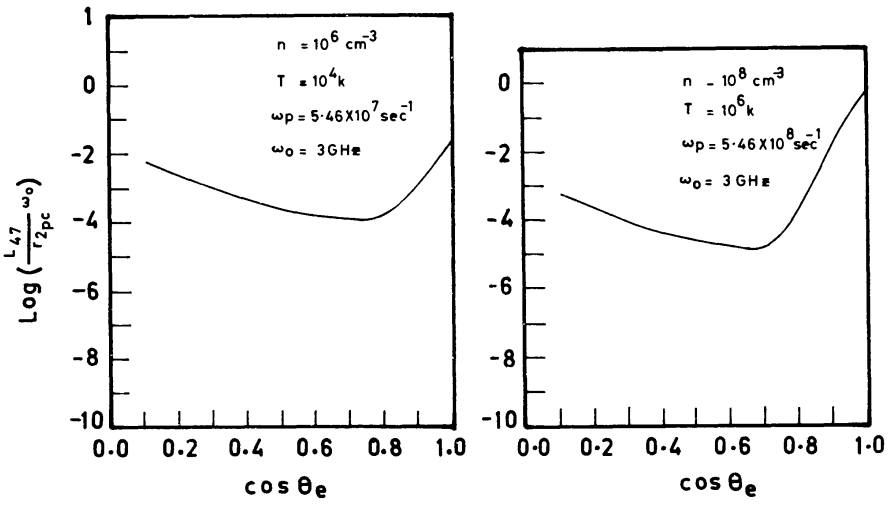

Figure 2. Variation of threshold luminosity with $\cos\theta_e$ at a fixed frequency $\omega_0 = 3$ GHz.

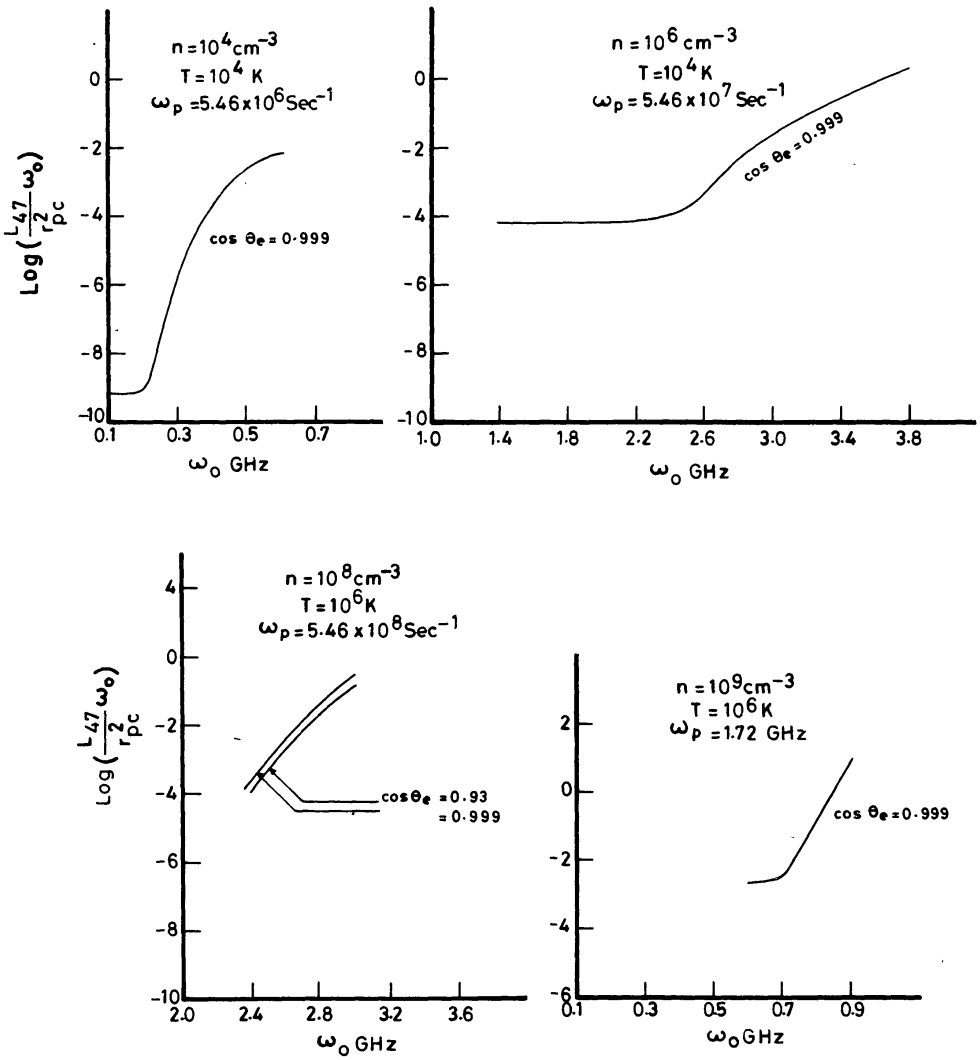

Figure 3. A plot of $(L_{47}\omega_0/r_{pc}^2)$ *vs* frequency ω_0 of the incident radiation for different parameters of the scattering plasma and $\alpha = 1$.

plasma parameters. It is seen that the Raman scattering can occur over a range of frequencies decided by the plasma parameters and the scattering angle for very reasonable values of the radio luminosity L. However, Raman scattering may not take place for very large and very small values of θ. The superluminal motion may appear to stop due to the increasing inefficiency of the Raman scattering to produce a virtual image. Raman scattering again becomes operative when the jet is about to complete a revolution and makes appropriate angles to the line of sight. But now, the resulting apparent motion will be towards the core, which has been reported though not yet confirmed in a couple of cases. In this scenario, the jet swings from one side of the core to the opposite side in about a rotation period of the radiation beam.

In reality, the scattering plasma may be in the form of clouds floating around the rotating radiation beam in the core, instead of being a continuous ring. The distribution may have different geometries: annular, disc, shell or filled sphere. Different perspectives of the plane of symmetry and the plane of the rotating beam are also possible. A choice of these can result in virtual images with several components,

possibly with diffuse haloes around them, exhibiting subluminal or superluminal motion. Sporadic increase in the incident luminosity would result in the brightening of different components at different times.

An attempt to fit observations with a two-component model leads to a large scatter in the plot of angular size of the source against time (Cohen & Unwin 1982). This has led to the suggestion that the observed source has several components. A model with several discrete clouds can give rise to a multi-component virtual image.

The stimulated Raman scattering is also a function of the angle between the electric vectors of the incident and scattered radiation. So, for a fixed value of the luminosity parameter (L_{47}/r_{pc}^2) and plasma parameters, one can calculate the amount of rotation that the electric vector of the scattered radiation had undergone with respect to the incident radiation.

4. Conclusion

The advantages of Raman scattering over any other incoherent process are (i) the scattered radiation has an intensity almost comparable to that of the incident because under the condition $\omega_0 \gg \omega_p$ very small amount of energy goes to the plasma waves (Figueroa *et al.* 1984), and thus the source does not diminish very much as it undergoes this apparent motion; and (ii) again because of $\omega_0 \gg \omega_p$ there is no significant spectral modification of the scattered radiation, and thus the characteristics of the real source are reproduced faithfully in the virtual source generated due to Raman scattering. Observations of the polarization differences between the core and the superluminally moving components will provide a test of the model.

Acknowledgements

The author is grateful to Prof. R. D. Blandford for suggesting this problem, to Prof. R. K. Varma, the referee, for pointing out that in the unrevised version a halo was produced instead of motion, and to Dr T. P. Prabhu for many very useful discussions during the revision of this paper.

References

Barnothy, J. M. 1965, *Astr. J.*, **70,** 666.
Blandford, R. D., McKee, C. F., Rees, M. J. 1977, *Nature*, **267,** 211.
Blandford, R. D., Konigl, A. 1979, *Astrophys. J.*, **232,** 34.
Cohen, M. H., Unwin, S. C. 1982, in *IAU Symp.* 97: *Extragalactic Radio Sources*, Eds D. S. Heeschen & C. M. Wade, D. Reidel, Dordrecht, p. 345.
Drake, J. F., Kaw, P. K., Lee, Y. C., Schmidt, G. 1974, *Phys. Fluids*, **17,** 778.
Figueroa, H., Joshi, C., Azechi, H., Ebrahim, N. A., Estabrook, K. 1984, *Phys. Fluids*, **27,** 1887
Krishan, V. 1988, *Mon. Not. R. astr. Soc.* **230,** 183.
Sanders, R. H. 1974, *Nature*, **248**, 390.
Scheuer, P. A. G. 1984, in *IAU Symp.* 110: *VLBI and Compact Sources*, Eds R. Fanti, K. Kellermann & G. Setti, D. Reidel, Dordrecht, p. 197.
Wilson, D. B. 1982, *Mon. Not. R. astr. Soc.*, **200,** 881.